Available online at www.sciencedirect.com

ScienceDirect

Energy Procedia 122 (2017) 787–792

Energy Procedia

www.elsevier.com/locate/procedia

CISBAT 2017 International Conference – Future Buildings & Districts – Energy Efficiency from Nano to Urban Scale, CISBAT 2017 6-8 September 2017, Lausanne, Switzerland

**Nano & Microstructured Materials for Renewable Energies (Solar Nano and Microtechnologies)**

# Development and characterization of electrochromic oxide and ion conductor deposited by reactive magnetron sputtering

D. Mansour[a]*, O. Bouvard[a], A. Schüler[a]

[a]*Solar Energy and Building Physics Laboratory (LESO-PB), Ecole Polytechnique Fédérale de Lausanne (EPFL)*

**Abstract**

In order to modulate the solar gains of a building, electrochromic windows can be used. To improve their durability, inorganic solid state electrolytes are considered. This work reports on the investigation of tungsten trioxide ($WO_3$) and lithium phosphorous oxynitride (LiPON) used as electrochromic oxide and solid state ion conductor respectively. The impacts of porosity on the optical and the electrochemical properties as well as the determination of ionic conductivity of LiPON are studied.
Electro-optical performances were studied by developing an in-situ experimental set-up allowing the measurement of the spectral transmittance during the electrochemical characterizations. The techniques of chrono-amperometry and simultaneous spectrophotometry were used to determine the coloration efficiency as well as the response times for coloration and bleaching of the $WO_3$ films. Electrochemical impedance spectroscopy was performed to investigate the electrochromic and electrolyte materials. The ionic conductivity was measured for LiPON sandwiched in metal-insulator-metal (MIM) cells.


Peer-review under responsibility of the scientific committee of the CISBAT 2017 International Conference – Future Buildings & Districts – Energy Efficiency from Nano to Urban Scale

*Keywords:* Electrochromism; tungsten oxide; lithium phosphorous oxynitride; magnetron sputtering; ionic conductivity; coloration efficiency; swiching time

* Corresponding author.
*E-mail address:* djamel.mansour@epfl.ch

1876-6102 
Peer-review under responsibility of the scientific committee of the CISBAT 2017 International Conference – Future Buildings & Districts – Energy Efficiency from Nano to Urban Scale
10.1016/j.egypro.2017.07.397

## 1. Introduction

Electrochromism is a phenomenon of reversible colour changes based on the electrochemical redox reactions in electrochromic materials. Properties such as direct transmittance, light transmittance, reflectance and absorption can be controlled. A solid-state electrochromic device works like a lithium ion micro battery. The cathode, tungsten trioxide, and the solid-state electrolyte, lithium phosphorous oxynitride, can be deposited by reactive magnetron sputtering [1-3]. According to Granqvist, increasing the total working pressure can modify the morphology of the $WO_3$ film and creates porosity [4,5]. It was shown that the working pressure influences strongly the stoichiometry of the $WO_3$ film [6]. Lithium phosphorous oxynitride or LiPON has received broad attention since its discovery by Bates and al. in 1992 [7]. This is mainly due to its high ionic conductivity, thermal and chemical stability and good optical properties [1-3,8]. Therefore, LiPON is not only a good candidate as a solid-state electrolyte used in batteries but also for electrochromic devices for the application in advanced glazing. This study consider two different aspects: one is the investigation on the impact of porosity of $WO_3$ film on the optical and the electrochemical properties and the other one is the determination of ionic conductivity of LiPON used as solid ion conductor film for the electrochromic materials. Using an inorganic electrolyte can improve the durability of the electrochromic device which is necessary for the use in buildings. Smart windows composed of electrochromic coating shall minimize the energy consumption of the building and provide the best daylight management.

## 2. Methods

### *2.1. Thin film deposition*

The tungsten trioxide ($WO_3$) films have been deposited on Indium Tin Oxide (ITO) coated glass substrate by using reactive magnetron sputtering. $WO_3$ coating was deposited from a 2-inch diameter metallic target of tungsten and a mixture of oxygen as reactive gas and argon gas for creating the plasma. The power applied to the target was 150 W from a DC power supply. The working pressure in the chamber during deposition was varied in order to obtain a dense and a porous sample.
The LiPON film was deposited by Radio Frequency magnetron sputtering from $Li_3PO_4$ 2-inch diameter target with an applied power of 100 W in pure nitrogen plasma. The working pressure during deposition was $4.9 \cdot 10^{-3}$ mbar. Metallic Al was deposited by magnetron sputtering to build metal-insulator-metal (MIM) cells Al/LiPON/Al, for electrical measurements of LiPON. The Al electrodes were deposited using a mask.

### *2.2. Optical properties*

Time-dependent transmittance measurements were performed in combination to electrochemical characterizations, described in the next paragraph, using a spectrophotometer (Zeiss diode array spectrometer). The transmission of samples was measured between 348 and 1602 nm. Above 1602 nm, the absorptance of the liquid electrolyte dominates. The transmittance spectra were weighted by the solar spectra, and by the spectral sensitivity of the eye, to determine the coefficient of solar direct energy transmission $\tau_e$, and visible light transmission $\tau_v$ respectively, according to EN410 [9]. As shown in Fig.1, the UV-visible-NIR light beam passes through an electrochemical cell and is collected by an optical fiber. The transmittance of the sample is calculated according to the reference measured through the electrochemical cell containing the liquid electrolyte but no sample. A spectrum is acquired every 7.36s.
Before electrochemical cycling, optical measurements were performed in the visible range using a Multispec 77400 spectrometer from ORIEL equipped with integrating sphere, to determine the transmittance and reflectance of the ITO/$WO_3$/LiPON multilayer sample as deposited.

### *2.3. Electrochemical characterisation*

For electrochemical techniques, cyclic voltammetry and chrono-amperometry were performed in a three-electrode electrochemical cell with a Bio-Logic SP-200 potentiostat/galvanostat**.** An $Ag/AgNO_3$ electrode cell was used as a reference electrode and a platinum wire as a counter electrode. The working electrodes were the ITO/$WO_3$ samples.

These electrodes were immersed in a parallelepiped cell containing the liquid electrolyte, 1M lithium perchlorate in propylene carbonate ($LiClO_4$-PC), as depicted in Fig.1.

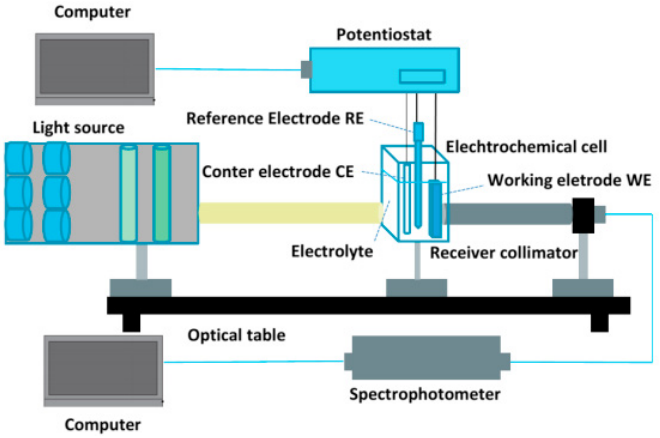


Fig.1. Schematic drawing of the setup used to perform electrochemical measurements in combination with transmittance measurements

In this work, 10 cycles of voltammetry (CV) are applied between -2.5 and 2.5 V at a scan rate of 25 mV/s. Note that a discoloration voltage 1.5 V vs. $Ag/AgNO_3$ is applied for 180 seconds before the cycles to start at the bleached state. In order to assess the performance of an electrochromic thin film, one needs to evaluate the intercalation level ($x$ in $Li_xWO_3$) which indicates the ability of the host material to receive ions, see Eq.1.

$$x = \frac{Q_{int} \cdot M}{e \cdot A \cdot d \cdot \rho \cdot N_A} \tag{1}$$

Where $Q_{int}$ is the inserted charge (in C) calculated as the integral of the current as function of time, $M$ is molar mass (in $g.mol^{-1}$), $e$ is elementary charge (in C). $A$ is the working electrode area (in $cm^2$), $d$ is the film thickness (in cm), $\rho$ the density of the film and $N_A$ is Avogadro's constant (in $mol^{-1}$).

The diffusion coefficient of the $Li^+$ cations ($D^+$) resulting from the maximum anodic current ($I_p$) is found using the Randles-Sevčik equation (Eq.2). [10]

$$I_p = 0.4463 \cdot n_e \cdot F \cdot A \cdot C_s \cdot \sqrt{\frac{n_e \cdot F \cdot v \cdot D^+}{R \cdot T}} \tag{2}$$

Where $n_e$ is the number of electrons participating in the electrochemical reaction, $F$ is the Faraday constant (units of in $C.mol^{-1}$), $C_s$ is the solution concentration (in $mol.cm^{-3}$), $A$ is the working electrode area (in $cm^2$), $v$ is the scan rate (in $mV.s^{-1}$), $R$ is the ideal gas constant (in $J.mol^{-1}K^{-1}$) and $T$ is the temperature (in K).

Chronoamperometry (CA) was performed for a duration 600 s per cycle. While four different of potential ranges were applied: (-2.5 ; 2.5 V), (-2.0 ; 2.0 V), (-1.5 ; 1.5 V) and (-1.0 ; 1.0 V). Using this method, one can also evaluate the coloration efficiency *(CE)*, calculated using equation in Eq.3.

$$CE = \frac{Ln\left(\frac{T_b}{T_c}\right)}{Q_{int}} \cdot A \tag{3}$$

Where $T_b$ is the light transmittance ($\tau_{v,b}$) or the solar direct transmittance ($\tau_{e,b}$) in the bleached state, $T_c$ is the light transmittance ($\tau_{v,c}$) or the solar direct transmittance ($\tau_{e,c}$) in the colored state.

Electrochemical impedance spectroscopy (EIS) characterizations of the all solid-state Al/LiPON/Al cells were performed to determine the ionic conductivity. Sinusoidal voltage amplitude of 10 mV was used and the measurement frequency range was 2 MHz to 100 Hz. The results, displayed in a Nyquist impedance plot, were fitted using the equivalent circuit method.

## 3. Results

Cyclic voltammograms curves of $WO_3$ deposited at different working pressures are presented in the Fig.2.a for the 5th cycle. The previous cycles activate the host material. It is known that electrochromic film is colored by charge injection $\mathbf{WO_3 + x\,(Li^+ + e^-) \rightarrow Li_xWO_3}$, in the bottom region where the current is negative, and a part of this charge is extracted $\mathbf{Li_xWO_3 \rightarrow WO_3 + x\,(Li^+ + e^-)}$ during the bleaching process in the top region, where the current is positive. From this last region, the anodic peak current $I_p$ can be determined. Fig.2.b and Fig.2.c show the sample in bleach and colored state. The film properties calculated from these voltammograms are shown in Table.1.

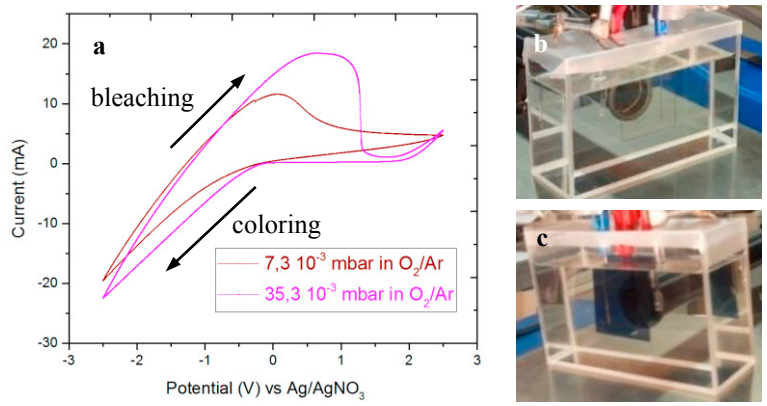


Fig.2. Electrochemical cell in three electrodes set- (a) Cyclic voltammograms for a scan rate of 25 mV/s for WO3 deposited at different pressures up (b) $WO_3$ sample in the bleached state, (c) $WO_3$ sample in the colored state

Table 1. CV parameters determined for a potential window of -2.5 / 2.5 V of the sample deposited at a low and high working pressure

| Average working pressure $10^{-3}$ (mbar) | $I_P$ (mA) | $D^+$ ($cm^2/s$) | $Q_{ext}$ (mC) | $Q_{int}$ (mC) | x (%) |
|---|---|---|---|---|---|
| 7,3 | 11.6 | $1.62 \cdot 10^{-12}$ | 1234.0 | -1179.7 | 24.4 |
| 35,3 | 18.4 | $3.03 \cdot 10^{-12}$ | 1456.5 | -1499.6 | 50.4 |

Larger current windows are observed when $P$ is increased from $7.3 \cdot 10^{-3}$ mbar (dense $WO_3$ film) to $35.3 \cdot 10^{-3}$ mbar (porous $WO_3$ film). $D^+$ represent the diffusion through the sample, a higher diffusion coefficient means that the ion can diffuse faster. In Table 1, we can see that $D^+$ is higher for the porous sample. $Q_{int}$ and $Q_{ext}$ are the inserted and extracted charge (in C), we can observe that the working pressure $P$ has a direct impact on the amount of inserted charge and thus on the intercalation level.

The results of *in situ* spectro-electrochemical experiments are represented as chronoamperometry combined to time-dependent transmittance measurements for UV-Vis-NIR wavelength. Fig.3. shows the solar direct energy transmission $\tau_e$ and the visible light transmission $\tau_v$ as function of time during four charging-discharging cycles. Fig.3. a shows the results on the dense $WO_3$ sample, it is observed that the magnitudes of $\tau_v$ and $\tau_e$ are smaller after the 1st cycle then increased slightly and becoming stable. Fig.3. b shows the results on the porous $WO_3$ sample, a reversible response for coloration and bleaching during electrochemical cycles is observed. The porous film exhibit decent performance with a coloration efficiency of 21,4 and 23,2 $cm^2/C$ for $\tau_e$and $\tau_v$ respectively. In contrast to this, the dense film showed lower coloration efficiency of 17,1 and 17,3 $cm^2/C$ for $\tau_e$and $\tau_v$ respectively. The difference between the bleached $T_b$ and colored $T_c$ normalized transmittance $(\Delta T)$ is increased with the increase of the working pressure. The switching time $\tau_{sw}$ is obtained for the samples, which is typically defined as the time to reach 90% of the maximum transmission modulation [10,11]. The films possess a longer switching time in the bleaching ($\tau_b =$ 206.1s) than in the coloration ($\tau_c$ = 51.5s) process.

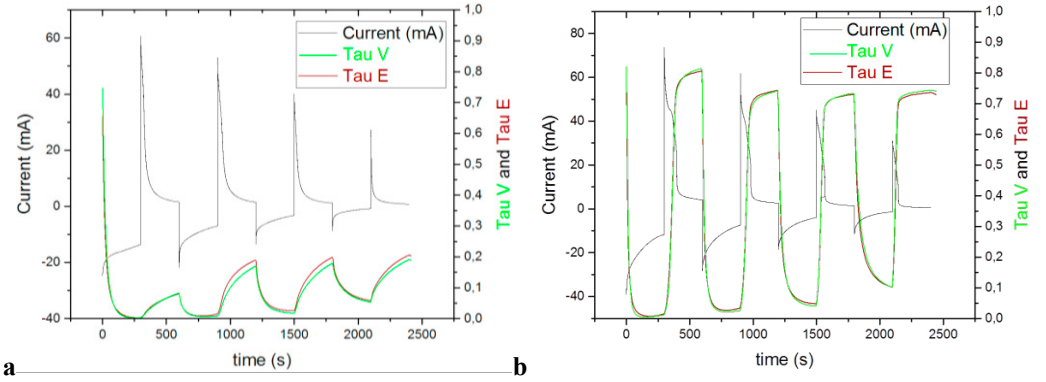


Fig. 3. Transmission variation combined with 4 CA cycles of the $WO_3$ at different potential applied: (a) Dense film and (b) Porous film

Fig. 4.a. depicts the spectral transmittance and reflectance of a $WO_3$/LiPON film. The as-deposited film shows a very good transparency with high transmittance. The transmittance spectrum averages approximately at 80% and the reflectance spectra at ~15% over the visible portion in the dry state. The oscillations in the graph of transmittance and reflectance are due to interference in the ITO and $WO_3$ as well as $WO_3$ and LiPON thin films.

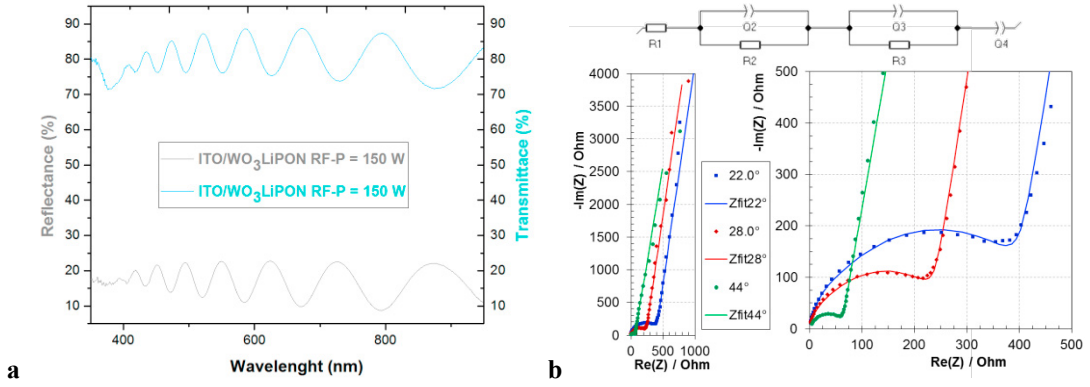


Fig. 4. (a) Transmittance and reflectance measurements of as-deposited of $WO_3$/LiPON film. (b) Electrochemical impedance spectra of Al/LiPON/Al measured for three temperatures (22, 28 and 44.2°C) and fitted using the equivalent circuit shown

Fig. 4.b. shows the Nyquist impedance plots of Al/LiPON/Al film obtained at different temperatures (22,0°; 28,0° and 42,2° C) for all frequencies and then zoomed on the high frequency part of the diagram. At all temperatures, the impedance spectra show curved shapes typical of RC circuits and then a straight line. The curved shape is at high frequencies and corresponds to the electrolyte. These results form a combined response related to the ionic conduction across the solid electrolyte layer and the charge transfer reaction at the electrode/solid-state electrolyte interface. The size of the curved shape decreases with increasing the temperature. We can observe that the three straight lines present the same slope at each temperature. The equivalent circuit that we use to fit EIS data is shown in Fig. 4.b. The resistance R1 represents the resistance of contacts and leads and corresponds to the intercept of the semicircle with the real axis at high frequency. The ionic conduction processes are represented by two pairs of resistor and capacitor in parallel at high and medium frequencies (R2/Q2 and R3/Q3), as well as a double-layer capacitance (Q4) at low frequency. The high frequency part is interpreted to indicate the bulk properties of the LiPON film [8]. The low frequency part, toward large real numbers, corresponds to the electrodes interface phenomena. The ionic conductivity $\sigma_i$ of LiPON in MIM cells, for a thickness of d=300 nm; has been calculated from the resistance R=R2+R3 measured by using Eq.4, A being the area of the electrode in contact with the solid electrolyte.

$$\sigma_i = d / R.A \tag{4}$$

The ionic conductivity of LiPON is found to increase ($8.71 \cdot 10^{-8} \rightarrow 1.48 \cdot 10^{-7} \rightarrow 5.74 \cdot 10^{-7}$ S·cm$^{-1}$) with increasing temperatures (22,0°→ 28,0°→ 42,2° C) and the activation energy has been calculated to be 0.3 eV.

## 4. Discussion

The inserted charge ($Q_{int}$) and consequently the intercalation level *(x)* of $Li^+$-cations in $Li_xWO_3$ (see Eq.1) are shown to be increased with an increase of the working pressure, it explains that the microstructure is being larger for porous $WO_3$ films, allowing a faster intercalation/deintercalation process. The diffusion coefficient of $Li^+$-cations ($D^+$) deduced from the anodic peak current ($I_P$) (see Eq.2) is increased at high working pressure, to confirm facilitated performances of this process. For $WO_3$ deposited at low pressure the magnitudes of optical modulation are getting too small. This behavior confirms that the film is too dense and $Li^+$-ions cannot be extracted after cycles. The switching time $\tau_{sw}$ is in the same range than most of the $WO_3$ EC devices on ITO substrates. Senevirathne et al [12] studied the ion migration path in $Li_2PO_2N$ and calculated that the vacancy migration path is approximately 0.4 eV while the interstitial migration path is approximately 0.9 eV. The measured activation energy of our LiPON sample was found to be 0.3 eV, this suggests that we would have a dominant vacancy migration path.

## 5. Conclusions

Transparent layers of amorphous $WO_3$ and LiPON have been deposited by reactive magnetron sputtering. The porosity of the tungsten oxide was changed by depositing it under two different working pressures. Cyclic voltammetry measurements were performed in order to assess the impact of porosity on the electrochemical properties. It has been found that the porous $WO_3$ film allows a faster and an easier intercalation/deintercalation process. Chrono-Amperometry measurements combined to transmittance measurements for UV-Vis-NIR wavelengths were performed in order to investigate the bleaching-coloration reversibility of the electrochromic layers. The porous film exhibits a shorter switching time and higher coloration efficiency and switching contrast than the dense film. The deposition of LiPON on top of $WO_3$ did not change the transparent aspect of $WO_3$ and therefore suggest that no or very limited diffusion of Li into $WO_3$ occurs during deposition. Finally, the ionic conductivity as well as energy activation was determined for our LiPON in MIM cells by using potentio-electrochemical impedance spectroscopy.

## Acknowledgment

This research has been financially supported by CTI within the SCCER FEEB&D (CTI.2014.0119).

## References

[1] S. Oukassi, C. G-Garampon, C. Dubarry, C. Ducros, R. Salot, All inorganic thin film electrochromic device using LiPON as the ion conductor. Solar Energy Materials & Solar Cells 145 (2016) 2–7
[2] S. Jee, M. Lee, H. S. Ahn, D. Kim, J. W. Choi, S. J. Yoon, S. C. Nam, S. H. Kim, Y. S. Yoon, Characteristics of a new type of solid-state electrolyte with a LiPON interlayer for Li-ion thin film batteries. Solid State Ionics 181 (2010) 902–906
[3] L. Kovalenko, O.V'yunov, A.Belous, F. Goutenoire, V. Gunes, O. Bohnke, Effect of Deposition Conditions On Microstructure of LiPON Films Obtained by RF Magnetron Sputtering. (2014) IEEE XXXIV (ELNANO)
[4] C. G. Granqvist, Electrocromics for smart windows: Oxide-based thin films and devices. Thin Solid Films 564, 1 (2014).
[5] C. G. Granqvist, Handbook of Inorganic Electrochromic Materials (Elsevier, Amsterdam, 1995)
[6] O. Bouvard, A. Krammer, A. Schüler, In situ core-level and valence-band photoelectron spectroscopy of reactively sputtered tungsten oxide films. Surface and Interface Analysis. (2016)
[7] J. B. Bates, N. J. Dudney, G. R. Gruzalski, R. A. Zuhr, A. Choudhury, C. F. Luck, Solid State Ionics 53-56 (1992) 647-654
[8] Nowak S, Berkemeier F, Schmitz G. Ultra-thin LiPON films – Fundamental properties and application in solid state thin film model batteries. Journal of Power Sources. (2015) 275:144–50.
[9] NF EN 410, Glass in building, Determination of luminous and solar characteristics of glazing. 2011. AFNOR
[10] H. Camirand, B. Baloukas, J. E. Klemberg-Sapieha, L. Martinu, In situ spectroscopic ellipsometry of electrochromic amorphous tungsten oxide films. Solar Energy Materials & Solar Cells 140 (2015) 77–85
[11] R. Batens, B.P. Jelle, A. Gustavsen, Properties, requirements and possibilities of smart windows for dynamic daylight and solar energy control in buildings: a state-of-art
[12] K. Senevirathne, C.S. Day, M.D. Gross, A. Lachgar, N.A.W. Holzwarth. A new crystalline LiPON electrolyte: Synthesis, properties, and electronic structure. Solid State Ionics. 233 (2013) 95–101.